

Lawrence Berkeley National Laboratory

Lawrence Berkeley National Laboratory

Title

DIFFUSION MODEL PREDICTIONS FOR KINETIC ENERGY, MASS, ANGULAR DISTRIBUTIONS AND gamma-RAY MULTIPLICITIES IN HEAVY ION INDUCED REACTIONS

Permalink

<https://escholarship.org/uc/item/7sn4g304>

Author

Moretto, L.G.

Publication Date

1977-08-01

Diffusion model predictions for kinetic energy, mass, angular distributions and Y-ray multiplicities in heavy ion induced reactions*

L. G. Moretto

The Department of Chemistry and Lawrence Berkeley Laboratory, University of California, Berkeley, California 94720, USA

Abstract: In the present formalism the diffusion along the mass asymmetry coordinate has been generalized by refining the treatment of the radial and angular motion necessary for an adequate reproduction of the kinetic energy and angular distributions. The radial potential is used to evaluate the radial force. The interaction time and the average penetration for each l -wave are estimated. The diffusion calculation is then carried out for the duration of the interaction time. The angular rotation during diffusion is calculated for each fragment on the basis of the tangential energy. The resulting average deflection function shows the deep inelastic rainbow observed experimentally. The rainbow angle moves from positive to negative angles with increasing bombarding energy. Good agreement is obtained for the average final kinetic energy as a function of angle. The calculated Z distributions become broader as the excitation energy increases. The angular distributions for individual fragments show the characteristic disappearance of the side peaking and the development of forward peaking as the distance in Z from the projectile increases. The calculated Z angular and Y-ray multiplicity distributions are successfully compared with the experimental data.

NOTICE: This report was prepared as an account of work sponsored by the United States Government. Neither the United States Government, neither the Energy Research and Development Administration, nor any of their contractors, subcontractors, or employees, makes any warranty, express or implied, or assumes any legal liability for the accuracy, completeness or usefulness of the information appearing in this report, except as may be stated in writing. It is to be understood that the use of the word "should" in this report is intended to indicate a recommendation or a course of action that is not mandatory.

Introduction

Heavy ion reactions have provided substantial evidence of relaxation mechanisms, associated with a number of collective degrees of freedom⁽¹⁾. The experimental evidence suggests a hierarchy of characteristic times in the relaxation of these modes. From faster to slower, one can list the neutron-to-proton ratio of the fragments, their relative motion, the fragment intrinsic rotation and the mass asymmetry of the system. The relaxation of the asymmetry mode extends well into times when all the previous modes have essentially reached equilibrium.

*This work has been partially supported by the Niels Bohr Institute, Copenhagen, and partially supported by the U.S. Energy Research and Development Administration.

It is useful to think of the system as a reaction intermediate or intermediate complex⁽²⁾ which, during its lifetime, undergoes equilibration processes which are interrupted at various stages of completion at the time of decay.

The dissipation of large amounts of kinetic energy into the internal degrees of freedom generates a thermal background which introduces brownian perturbations in the collective motions. One is then led to believe, from this and other experimental evidence, that the time evolution, at least for the slower modes, may be diffusive in its nature and describable in terms of the Master Equation or its equivalent, the Fokker-Planck equation^(2,3).

It is the purpose of this paper to present a simple model which tries to describe specifically the time evolution of the mass asymmetry degree of freedom. As it is not possible to experimentally isolate this particular mode from all the others, the model must account for them to some extent.

A brief summary of the relevant physical facts follows⁽¹⁾. The experimental data are consistent with complete dissipation of the radial kinetic energy, while the tangential kinetic energy seems to be dissipated to a lesser degree. This has the consequence that for large impact parameters there is less energy relaxation than for small impact parameters.

There is some indication that the interaction time increases with increasing radial velocity^(1,4), which shows that such a time arises from a dynamical rather than a statistical mechanism. Such a dependence is inferred from the increase of the mass or charge distribution widths with bombarding energy and from the decrease of the same widths at constant energy with increasing angular momentum. Of course the alternative explanation of such a feature may lie in the dependence of the diffusion form factor upon radial penetration. The two explanations are not mutually exclusive as will be seen below.

The gross angular distribution is characterized by a rainbow (deep inelastic rainbow) which moves from positive to negative angles as the

energy (and the lifetime) increases. As this occurs, the angular distribution evolves from side-peaked to forward-peaked⁽¹⁾. Again the overall effect may be due to an increase in lifetime as well as in an increase in the angular velocity resulting from the angular momentum increase and in an average decrease of the moment of inertia with increasing average radial penetration.

A simple correlation can be established between the experimentally detected short and long interaction time patterns and the ratio E/B of the entrance channel kinetic energy and the interaction barrier. For $E/B < 1.5$ we observe the short interaction time regime, characterized by side-peaked angular distributions and narrow mass or charge distributions peaked at the projectile A, or Z. For $E/B > 1.5$ one enters the long interaction time regime, with forward-peaked angular distributions and very broad charge or mass distributions.

A most interesting feature, strongly supporting the diffusion picture, is the dependence of the angular distribution upon the mass or charge of the emitted fragment^(1,4). If the gross distribution is forward-peaked, the individual fragment angular distribution becomes less forward-peaked as the distance in Z from the projectile increases. If the gross angular distribution is side-peaked, the individual fragment angular distribution evolves from side-peaked to forward-peaked as the distance in Z from the projectile increases, as can be seen in fig. 3. These features are due to the progressive time delay introduced by diffusion in populating configurations farther and farther away from the entrance channel configuration.

It is this set of properties that the present theory shall try to reproduce.

The diffusion equations

We assume that the intermediate complex has a shape close to that of

two touching fragments. Charge to mass equilibration is assumed to be a rather fast process, so that the asymmetry of the system can be characterized by the mass or by the charge of one of the two fragments. We further assume that the time evolution along the asymmetry coordinate is diffusive in nature and describable in terms of the Master Equation:

$$\dot{\phi}(Z,t) = \int dz' [\Lambda(Z,z')\phi(z') - \Lambda(z',Z)\phi(Z)] \quad (1)$$

where $\phi(Z,t)$, $\dot{\phi}(Z,t)$ are the populations of the configurations characterized by the atomic number Z of one of the fragments, and their time derivative at time t ; and $\Lambda(Z,z')$, $\Lambda(z',Z)$ are the macroscopic transition probabilities.

If in eq. (1) one writes: $Z' = Z + h$ and all the quantities are expanded about Z in powers of h , one obtains to lower order:

$$\dot{\phi}(Z,t) = -\frac{\partial}{\partial Z} \left[\mu_1 \phi \right] + \frac{1}{2} \frac{\partial^2}{\partial Z^2} \left[\mu_2 \phi \right] \quad (2)$$

which is the well-known Fokker-Planck equation⁽⁵⁾. The quantities μ_1 and μ_2 are the first and second moment of the transition probabilities:

$$\mu_1 = \int h \Lambda(Z,h) dh \quad ; \quad \mu_2 = \int h^2 \Lambda(Z,h) dh \quad (3)$$

The Fokker-Planck equation has simple analytical solutions when μ_1 , μ_2 are constant and for the initial condition $\phi(Z_0, 0) = \delta(Z - Z_0)$:

$$\phi(Z,t) = (2\pi\mu_2 t)^{-1/2} \exp - [Z - (Z_0 + \mu_1 t)]^2 / 2\mu_2 t \quad (4)$$

Notice that the centroid of the gaussian moves with velocity μ_1 which can be related to the driving force $F = -V'_2$ and to the friction coefficient K by the relation: $K = \mu_1/F$.

An analytical solution is also available when the force is harmonic or:

$$V'_2 = \frac{c}{2} (Z - Z_{sym})^2 = \frac{1}{2} ch^2;$$

the solution is:

$$\phi(h,t) = c^{1/2} \left[2\pi T \left(1 - \exp \frac{2ct}{K} \right) \right]^{-1/2} \exp - \frac{c[h-h_0 \exp - ct/K]^2}{2T(1-\exp-2ct/K)} \quad (5)$$

where we have made use of the Einstein relation $\mu_1/\mu_2 = -V_Z^1/2T$ and T is the temperature.

The transition probabilities

From general phase space considerations one can consider the following ansatz for the transition probabilities (2):

$\Lambda(Z, Z') = \lambda(Z, Z') \rho_Z = \kappa f \rho_Z / (\rho_Z \rho_{Z'})^{1/2}$, where $\lambda(Z, Z')$ is the microscopic transition probability, ρ_Z is the final state density, κ is a particle flux and f is the window area between the two fragments. This can be rewritten as

$$\Lambda(Z, h) = \kappa f \exp - V_Z^1 h / 2T \quad (6)$$

The Fokker-Planck coefficients can then be calculated:

$$\mu_1 = -2\kappa f \sinh V_Z^1 / 2T \approx -\kappa f V_Z^1 / T ; \mu_2 = 2\kappa f \cosh V_Z^1 / 2T \approx 2\kappa f \quad (7)$$

which for large T satisfy the Einstein relation.

Such an ansatz implies for the friction coefficient: $K = \frac{T}{\kappa f}$.

Alternatively if the particle transfer between two fragments with chemical potential differing by an energy $a = V^1 h$ is considered, one can write:

$$\Lambda(Z, h) = Ag \int \frac{d\epsilon}{1 + \exp(\epsilon - a)/T} \left(1 - \frac{1}{1 + \exp \epsilon/T} \right) = \frac{Ag V_Z^1 h}{1 - \exp - V_Z^1 h/T} \quad (8)$$

where A is some strength constant and g the average single particle level density. The final result is:

$$\mu_1 = -Ag V_Z^1 ; \mu_2 = Ag V_Z^1 \coth V_Z^1 / 2T \approx 2 Ag T \quad (9)$$

again satisfying the Einstein relation. The friction coefficient is: $K = \frac{1}{Ag}$.

The two approaches lead to different results, namely the first predicts a friction coefficient proportional to the temperature, the second to a constant.

Other approaches described in literature^(3,5) lead to friction coefficients with a temperature dependence intermediate between the two extreme cases described above.

The diffusion constant

In eq. (7) the quantity κf can be considered a form factor for the transition probability, which should depend upon the overlap between the two fragments. If one takes the idea of particle transfer seriously, it is possible to write such a quantity, which is a particle transfer rate, as suggested by Randrup⁽⁶⁾:

$$\kappa f \equiv \int n \, d\sigma = 2\pi n_0 \bar{R} b \psi(\zeta) \quad (10)$$

where n_0 is the particle flux in nuclear matter at saturation density, $\bar{R} = \frac{C_1 C_2}{C_1 + C_2}$ is a reduced radius expressed in terms of the central radii of the two fragments, b is the skin thickness and $\psi(\zeta)$ is a universal function depending upon the separation between the sharp surface of the two fragments in units of the surface thickness. This approach neatly factors out the geometrical features of the problem.

The asymmetry potential energy

In general, the potential energy of the intermediate complex as a function of Z can be written as

$$V(Z, \ell) = V_{LD}(Z) + V_{LD}(Z_T - Z) + V_{Prox}(Z, \ell) + V_{Coul} + V_{Rot} \quad (11)$$

where ℓ is the total angular momentum, V_{LD} represent the liquid drop energies of the two fragments, and V_{Prox} is the nuclear interaction or proximity energy⁽⁸⁾.

The total potential V depends on the fissionability of the system x , on ℓ and on the distance between centers D . At low values of all of these parameters, V monotonically increases from $Z = 0$ to Z_{sym} where it reaches a maximum. As x , ℓ , D increase, the second derivative at Z_{sym} goes through zero and changes sign: thus for large values of these parameters,

V initially increases with Z, it reaches a maximum at some intermediate value of Z; it then decreases until it reaches a minimum at Z_{sym}.

The driving force which arises from this potential depends dramatically on the entrance channel asymmetry, as well as on x, l, D. It may either drive the system towards symmetry or towards extreme asymmetries. For a reaction like 600 MeV Kr + Au the driving force is in the direction of symmetry most of the time. In fact, the potential energy vs mass asymmetry for this and similar reactions can be approximated by a parabola. The knowledge of the l-dependent second derivative at the minimum and of the position of the injection point allows us to use an approximate analytical solution (eq. 5) to the Master Equation, thus greatly simplifying the calculations.

The radial and tangential motion

Both the diffusion constant and the asymmetry potential energy depend upon the distance between the two fragments. This distance is controlled by the radial motion of the system. Furthermore the extent to which the diffusion proceeds depends upon the interaction time. One needs then to study the radial motion in some detail. Unfortunately such dynamical studies available in literature appear to be inadequate for our purposes. We shall therefore limit ourselves to an extremely simplistic treatment which, however, respects the experimental evidence closely.

The radial potential can be written as:

$$V(D) = V_{\text{Prox}} + \frac{Z(Z_T - Z)e^2}{D} + \frac{\hbar^2 l^2}{2\mathcal{I}(l)} \tag{12}$$

$\mathcal{I}(l)$ being an appropriate moment of inertia.

It is not very clear how much the fragments must interpenetrate before the above equation breaks down. This makes it difficult to formulate the dynamical problem which, among other things should give the time dependence of the radial penetration of the two fragments $x(t, l)$ and the average interaction

time $\tau(\ell)$. Such a problem is unfortunately far from settled. For the present we shall just use the above potential to calculate the average force $F_R(\ell)$ at the interaction distance D_{int} : $F_R(\ell) = \partial V(D)/\partial D|_{D_{int}}$. From the knowledge, at interaction radius, of the reduced mass μ , of the radial velocity v_R and of the radial force F_R for each ℓ value, one can introduce the following two ansatz for the interaction time τ and the average penetration \bar{x} :

$$\tau(\ell) = \frac{2\mu v_R}{F_R} = \frac{2\sqrt{2\mu(E-B)}}{F_R} \left(1 - \frac{\ell^2}{\ell_{max}^2}\right)^{1/2}; \quad \bar{x}(\ell) = \frac{\alpha}{2} \frac{\mu v_R^2}{F_R} \quad (13)$$

For relatively small radial velocities, the functional form of the interaction time depends little upon the radial friction. The same cannot be said for the average penetration. In order to evaluate the latter we rely on a free parameter α . When better dynamical calculations become available it will be a trivial matter to substitute the ansatz in eq. 13 with more reliable expressions.

The diffusion along the asymmetry coordinate is then allowed to proceed with a form factor dependent upon $\bar{x}(\ell)$ for a time $\tau(\ell)$.

The tangential motion is treated assuming for the equation of motion the simple form:

$$F_T = \mu\gamma(\omega_0 - \omega_{Rig})$$

where ω_0 and ω_{Rig} are the two limiting orbital angular velocities corresponding to sliding and sticking. We then obtain for the angular velocity

$$\omega - \omega_{Rig} = (\omega_0 - \omega_{Rig})e^{-\gamma t}$$

and for the angle of rotation during the interaction time:

$$\theta = \omega_{Rig} t + \gamma^{-1}(\omega_0 - \omega_{Rig})(1 - \exp - \gamma t)$$

Such a formulation allows us to evaluate the exit channel kinetic energy.

The overall angle of rotation is calculated by adding the Coulomb orbit contribution from the entrance and exit channel.

All the equations are trivially modified for deviations from the entrance channel asymmetry.

The constant γ is chosen such as to approximately reproduce the mean kinetic energies as a function of angle assuming that all of the radial energy is lost.

Results of the calculations

The interaction times calculated for the reaction Au + Kr at three energies are shown in fig. 1a as a function of angular momentum. There is good experimental evidence for the angular momentum dependence predicted by our ansatz. It is interesting to notice the rather mild average increase in lifetime with increasing bombarding energy. In Fig. 1b the average deflection function is shown. Notice the well pronounced deep inelastic rainbow which moves from positive to negative angles as the bombarding energy increases. The 600 MeV curve, predicting a rainbow angle of about 50° is in excellent agreement with experiment. The movement of the rainbow angle towards smaller and eventually negative angles results from the combination of three factors: i) increasing lifetime; ii) increasing angular momentum; iii) decreasing average moment of inertia due to the increasing average penetration. In figs. 2a,b the calculated angle-integrated Z distributions are compared with experiment for the reactions Au + Kr and Ta + Kr at 620 MeV⁽¹⁾. The agreement is reasonable over more than two orders of magnitude. Some of the apparent discrepancies arise from the fact that the experimental angular distributions have been integrated over a fixed angular range. In figs. 4a and b, examples of the angular distributions for fragments of various Z are shown for both reactions. The theory nicely tracks the experiment in predicting forward peaked angular distributions at small Z's which develop into side-peaked angular distributions close to the projectile. For Z's above the projectile,

the angular distributions slowly lose their side peak and return forward peaked. The satisfactory reproduction of both the Z distributions and the angular distributions shows that the calculated dependence of the interaction times and of the diffusion constant upon angular momentum and radial velocity is reasonably good.

There is an additional confirmation of the validity of the diffusion model. The intrinsic angular momenta for each asymmetry have been studied by measuring the γ -ray multiplicities as a function of Z⁽⁸⁾. Our model can readily predict the total average angular momentum for a given Z. Its partition between orbital and intrinsic components depends on details of the exit channel shape that the present model does not predict explicitly. However we can assume an arbitrary shape, like two touching rigidly rotating spheres in order to calculate the angular momentum partition, well realizing that this assumption will completely fail close to the projectile where rigid rotation is certainly not attained, not even in our model. Rigid rotation is most likely a good approximation two or three Z units away from the projectile. In fig. 3 the estimated multiplicities and the corresponding widths are shown together with the experimental data⁽⁸⁾. The experimental data are corrected for the sequential fission occurring in the heavy fragment. The rise of the multiplicity at low Z's, expected for rigid rotation at constant angular momentum, is not seen in the calculation nor in the experiment. The reason lies in the driving force towards symmetry, much stronger at high than at low angular momentum. The diffusion process therefore selects out low angular momenta to populate the low Z configurations with the consequent low values of the γ -ray multiplicity.

There are two puzzling and possibly related difficulties. The first is the wrong dependence upon Z predicted for the γ multiplicity. The second is the nearly isotropic distribution of γ -rays as a function of the angle measured from an axis perpendicular to the reaction plane, rather than the

expected $W(\theta) \propto (1 - \cos^4 \theta)$ for stretched E2 transitions. The solution of the puzzle lies presumably in the depolarizing effect of dynamically generated angular momentum in the deep inelastic process.

In conclusion it appears that the present model is able to reproduce in a near quantitative way a large amount of the new features associated with deep inelastic processes and that a greater and more profound effort is necessary in order to describe the complex dynamical features associated with the radial and tangential motion.

References

- (1) For a more complete review on this subject see: L. G. Moretto and R. Schmitt. Journal de Physique C5 no. 11, 37 (1976), 109 and references therein: J. Galin, *ibid.*, C5 no 11, 37 (1976), 83
- (2) L. G. Moretto and J. S. Sventek: Phys. Lett. B58 (1975), 26
- (3) W. Nörenberg: Z. Physik A274 (1975), 241
- (4) L. G. Moretto, B. Cauvin, P. Glässel, R. Jared, P. Russo, J. Sventek and G. Wozniak: Phys. Rev. Lett. 36(1976), 1163
- (5) W. Nörenberg, Journal de Physique C5, no. 11, 37(1976), 141
- (6) J. Randrup: Proceedings of the International Workshop on Gross Properties of Nuclei and Nuclear Excitations, AED-Conf. 77-017-001, Hirschegg 1977
- (7) J. Blocki, J. Randrup, W. J. Swiatecki and C. F. Tsang: L3L 5014 (1976)
- (8) Preliminary results from L. G. Moretto and Diamond-Stephens groups, Berkeley

Figure Captions

- Fig. 1 Top. Dependence of the interaction time upon angular momentum at three bombarding energies for the reaction Au + Kr. Bottom. Average deflection functions for the same bombarding energies.
- Fig. 2 Angle integrated Z distributions for the reaction Au + 600 MeV Kr (a) and for Ta + 620 MeV Kr (b). The dots are the experimental points and the solid line the theoretical calculation.
- Fig. 3 Angular distributions of fragments of selected Z for the reaction Au + 600 MeV Kr (a) and for Ta + 600 MeV Kr (b). The dots are the experimental points and the solid lines the theoretical calculations.
- Fig. 4 Experimental and theoretical γ -ray multiplicities as a function of Z. The large band represent the theoretical width ($\pm \sigma$) which is also plotted in the lower part of the figure.

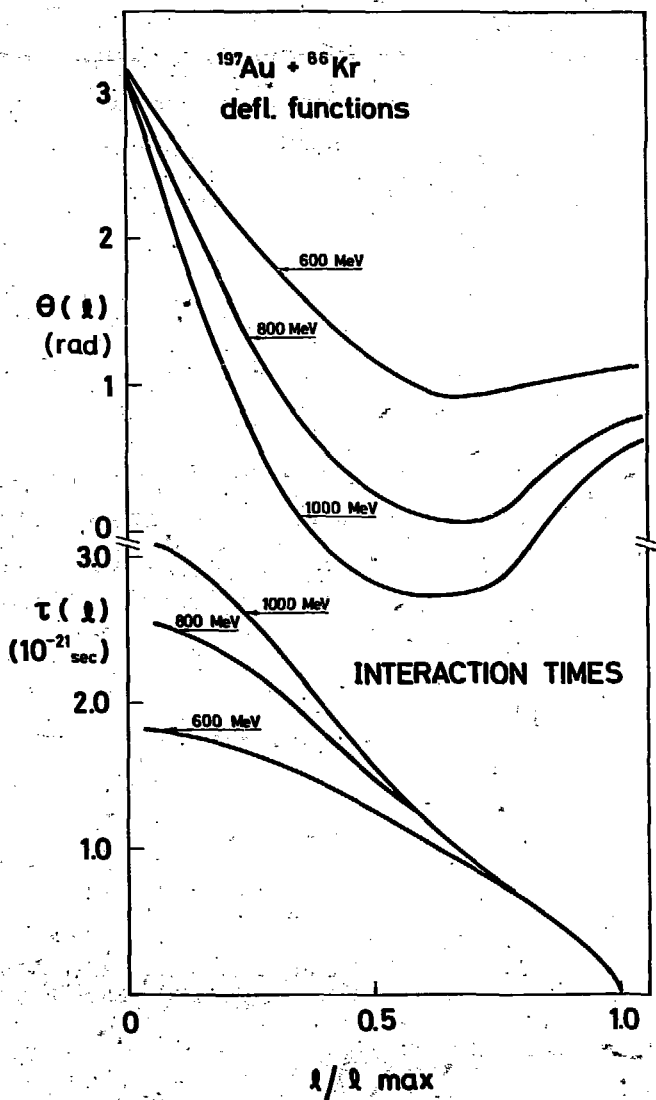
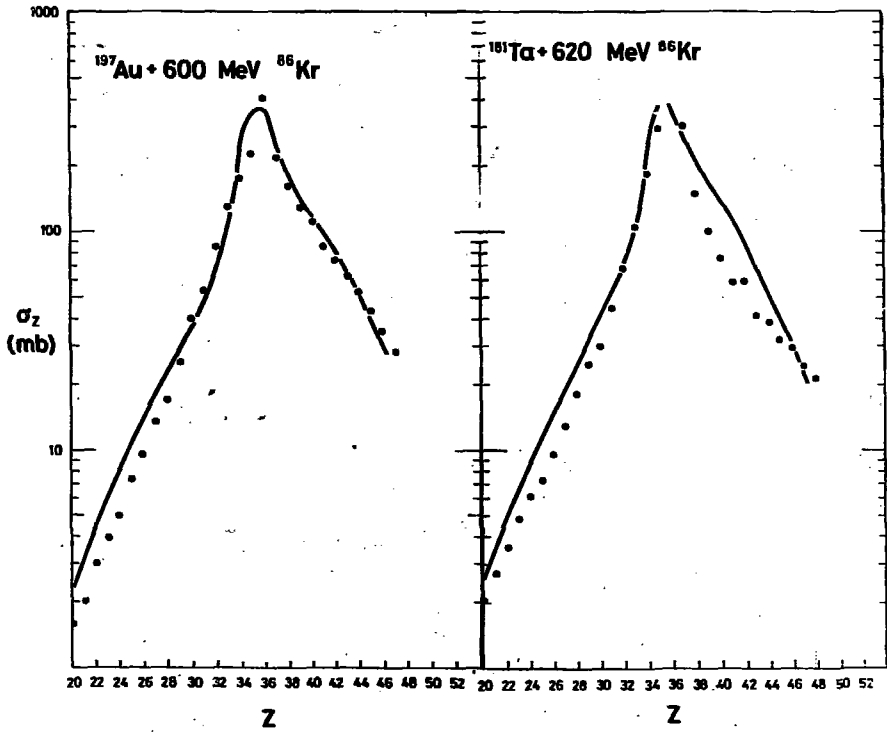


Fig. 1



XBL 778-8817

Fig. 2a

Fig. 2b

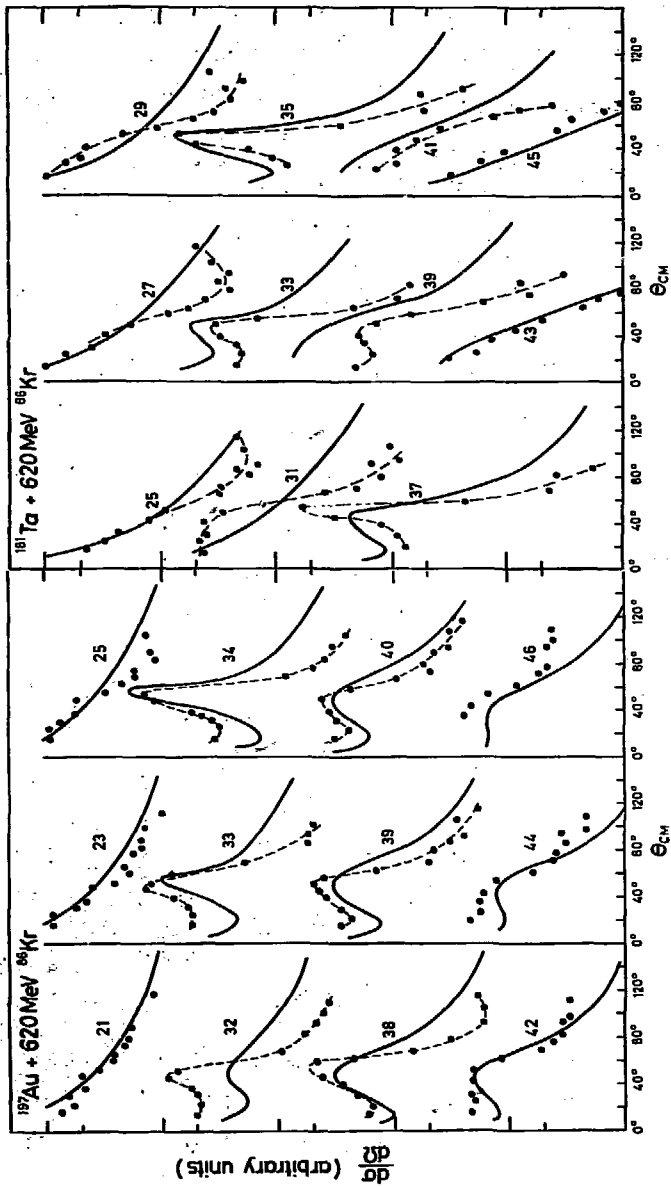


Fig. 3a

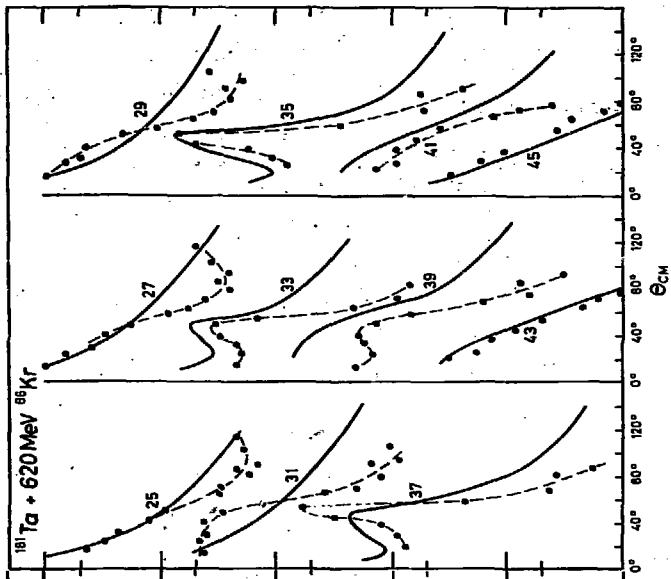


Fig. 3b

XBL 778-9508

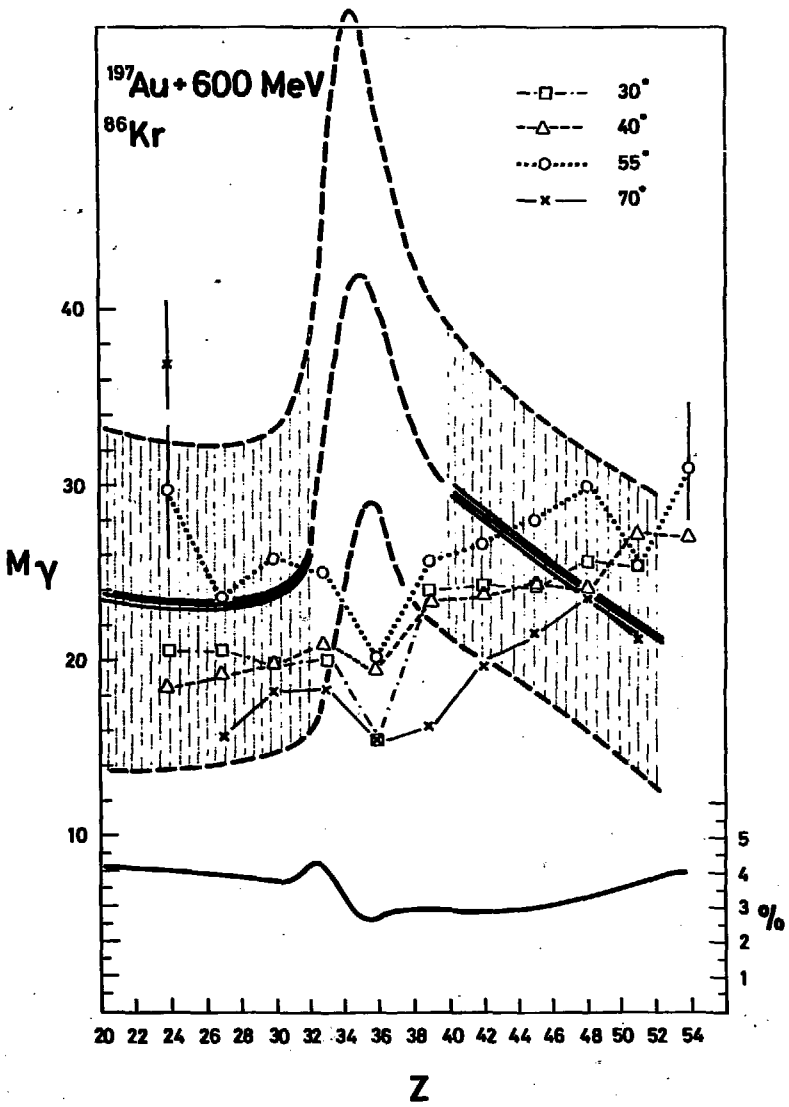


Fig. 4